


# Enhanced mechanical squeezing in an optomechanical system via backward stimulated Brillouin scattering

Shan-Shan Chen(陈珊珊), Yi-Long Xie(谢亦龙), Jing-Jing Zhang(张京京), Na-Na Zhang(张娜娜), Yong-Rui Guo(郭永瑞), Huan Yang(杨桓), and Yong Ma(马勇)

**Citation:**Chin. Phys. B, 2025, 34 (**1**): 014201. DOI: 10.1088/1674-1056/ad8cc0
Journal homepage: http://cpb.iphy.ac.cn; http://iopscience.iop.org/cpb

**What follows is a list of articles you may be interested in**

---

## Effects of cross-Kerr coupling on transmission spectrum of double-cavity optomechanical system

Li-Teng Chen(陈立滕), Li-Guo Qin(秦立国), Li-Jun Tian(田立君), Jie-Hui Huang(黄接辉), Nan-Run Zhou(周南润), and Shang-Qing Gong(龚尚庆)
Chin. Phys. B, 2024, 33 (**6**): 064204. DOI: 10.1088/1674-1056/ad2507

## Enhancement of the group delay in quadratic coupling optomechanical systems subjected to an external force

Jimmi Hervé Talla Mbé, Ulrich Chancelin Tiofack Demanou, Christian Kenfack-Sadem, and Martin Tchoffo
Chin. Phys. B, 2023, 32 (**12**): 124202. DOI: 10.1088/1674-1056/accc80

## Tunable phonon-atom interaction in a hybrid optomechanical system

Yao Li(李耀), Chuang Li(李闯), Jiandong Zhang(张建东), Ying Dong(董莹), and Huizhu Hu(胡慧珠)
Chin. Phys. B, 2023, 32 (**4**): 044213. DOI: 10.1088/1674-1056/acb9ea

## Quantum properties of nonclassical states generated by an optomechanical system with catalytic quantum scissors

Heng-Mei Li(李恒梅), Bao-Hua Yang(杨保华), Hong-Chun Yuan(袁洪春), and Ye-Jun Xu(许业军)
Chin. Phys. B, 2023, 32 (**1**): 014202. DOI: 10.1088/1674-1056/ac7206

## Nonreciprocal coupling induced entanglement enhancement in a double-cavity optomechanical system

Yuan-Yuan Liu(刘元元), Zhi-Ming Zhang(张智明), Jun-Hao Liu(刘军浩), Jin-Dong Wang(王金东), and Ya-Fei Yu(於亚飞)
Chin. Phys. B, 2022, 31 (**9**): 094203. DOI: 10.1088/1674-1056/ac6499

---

# Enhanced mechanical squeezing in an optomechanical system via backward stimulated Brillouin scattering

Shan-Shan Chen(陈珊珊)[1], Yi-Long Xie(谢亦龙)[1], Jing-Jing Zhang(张京京)[1], Na-Na Zhang(张娜娜)[1], Yong-Rui Guo(郭永瑞)[1], Huan Yang(杨桓)[1,†], and Yong Ma(马勇)[1,2,‡]

[1] *School of Optoelectronic Engineering, Chongqing University of Posts and Telecommunications, Chongqing* 400065, *China*
[2] *China Electronics Technology Group Corporation* 44*th Research Institute, Chongqing* 400065, *China*

(Received 18 September 2024; revised manuscript received 23 October 2024; accepted manuscript online 30 October 2024)

We investigate theoretically the enhancement of mechanical squeezing in a multimode optomechanical system by introducing a coherent phonon–photon interaction via the backward stimulated Brillouin scattering (BSBS) process. The coherent photon–phonon interaction where two optical modes couple to a Brillouin acoustic mode with a large decay rate provides an extra channel for the cooling of a Duffing mechanical oscillator. The squeezing degree and the robustness to the thermal noises of the Duffing mechanical mode can be enhanced greatly. When the Duffing nonlinearity is weak, the squeezing degree of the mechanical mode in the presence of BSBS can be improved by more than one order of magnitude compared with that in the absence of BSBS. Our scheme may be extended to other quantum systems to study novel quantum effects.

**Keywords:** mechanical squeezing, optomechanical system, backward stimulated Brillouin scattering, Duffing nonlinearity

**PACS:** 42.50.Lc, 42.50.–p, 42.50.Pq

**DOI:** 10.1088/1674-1056/ad8cc0 **CSTR:** 32038.14.CPB.ad8cc0

## 1. Introduction

Stimulated Brillouin scattering (SBS)[1–3] is an important nonlinear optical effect in the field of laser physics. SBS describes a coherent interaction between light and traveling acoustic wave, which originates from the electrostriction and photoelastic effects. This emerging subject leads to some remarkable and interesting topics, such as high coherence lasers,[4–7] Brillouin gyroscope[8] and Brillouin cooling.[9] Forward stimulated Brillouin scattering (FSBS)[9–12] and backward stimulated Brillouin scattering (BSBS)[13–16] have been research hotspots in recent years. In the BSBS, a Stokes optical signal is generated when a pump light photoelastically backscatters from a traveling acoustic wave. The remaining pump light and the Stokes optical signal electrostrictively excite the acoustic wave at the beat frequency of two optical signals. The wave vector conservation leads to the emergency of an acoustic mode at high frequency. In contrast to the BSBS, the Stokes optical signal in the FSBS copropagates with the forward-scattered pump light and the wave vector conservation results in a much lower acoustic frequency. The higher resonance frequency and the larger mechanical decay rate[13–16] of the acoustic mode in the BSBS hold immense promise for quantum control. First, a high-frequency acoustic mode enables low thermal occupation, the effect of the thermal noises on the quantum effect can be reduced. Second, a large mechanical decay rate is favorable for the control of the optical and mechanical quantum states, the related theoretical and experimental schemes have been reported in quantum-limited amplification,[17] the enhancement of the optomechanical entanglement and cooling,[18] and dissipatively controlled optomechanical interaction.[19] The proposal of these schemes opens the door to the application of BSBS in the field of cavity optomechanics. Recently, BSBS has been used to effectively enhance the optomechanical cooling and amplification of the target's mechanical oscillations,[19] and the investigation of the quantum properties based on the optomechanical system (OMS) via BSBS is attracting increasing attention.

The OMS,[20–24] where an optical field is coupled to a mechanical oscillator via radiation pressure force, is an important platform in quantum information processing. The fundamental study of the OMS includes optomechanically induced transparency,[25–27] mechanical squeezing,[28–30] ground-state cooling of the mechanical oscillator,[31–33] and so on. The phonon–photon interaction in the OMS arises from the radiation pressure force, while the electrostrictive force determines the generation of the phonon–photon interaction in the BSBS. The combination of cavity optomechanics and BSBS provides new opportunities for the quantum control of the phonon at the quantum level. The quantum squeezing of the mechanical mode has been at the center of many important developments in cavity optomechanics due to its potential applications in improving the precision of quantum measurement and

†Corresponding author. E-mail: yanghuan@cqupt.edu.cn
‡Corresponding author. E-mail: mayong@cqupt.edu.cn

© 2025 Chinese Physical Society and IOP Publishing Ltd. All rights, including for text and data mining, AI training, and similar technologies, are reserved.

continuous-variable quantum-information processing.[34–36] Mechanical squeezing based on the OMS can be achieved via many methods, including squeezing transfer between a cavity driven by a squeezed optical field and a mechanical mode,[37,38] the reservoir engineering technique,[39–41] and periodic amplitude modulation of the driving laser.[29,42–44] Ground-state cooling of a mechanical oscillator is the premise of the generation of mechanical squeezing. With the proposal of cooling a mechanical oscillator by using a Brillouin acoustic mode with high frequency and large decay rate in BSBS,[19] BSBS is expected to be used for the preparation of a strong quantum squeezing of the mechanical mode.

In this paper, we propose a scheme to enhance the quantum squeezing of the mechanical mode based on an OMS via BSBS. We find that, when the effective frequency detuning of the Brillouin acoustic mode and the phonon–photon coupling via the BSBS process are chosen properly, the introduction of phonon–photon interaction via the BSBS process provides a cooling channel for the target mechanical oscillator and the squeezing degree of the mechanical mode can be improved effectively. For a weak Duffing nonlinearity, the squeezing degree of the mechanical mode can be improved by more than one order of magnitude due to BSBS, and a strong mechanical squeezing which surpasses the 3 dB limit can be achieved. Our scheme provides a good theoretical guidance for studying more interesting quantum effects based on an optomechanical cavity.

This paper is organized as follows. In Section 2, we describe the multimode optomechanical model and obtain the linearized Hamiltonian. We study the effect of the phonon–photon interaction via the BSBS process on the steady-state position variance of the mechanical mode in Section 3, and we discuss the feasibility of the experiment and give a summary in Section 4.

## 2. Theoretical model

We consider a multimode OMS in which two optical modes $\hat{a}_1$ with frequency $\omega_1$, $\hat{a}_2$ with frequency $\omega_2$ couple to a traveling acoustic mode $\hat{b}$ with frequency $\omega_b$ via the BSBS process, and a Duffing mechanical oscillator $\hat{c}$ with frequency $\omega_{\rm m}$ and nonlinear amplitude $\eta$ couples to two optical modes $\hat{a}_1,\hat{a}_2$ simultaneously via the radiation pressure force. In the BSBS, as shown in Fig. 1, the triple-resonant BSBS occurs when the momentum conservation $|k_{\hat{a}_1}|+|k_{\hat{a}_2}|=|k_{\hat{b}}|$ and energy conservation $E_{\hat{a}_1}=E_{\hat{a}_2}+E_{\hat{b}}=\hbar\omega_1=\hbar\omega_2+\hbar\omega_b$ are both satisfied. The Hamiltonian of the full system can be described as ($\hbar=1$)

$$\hat{H}_{\rm T}=\hat{H}_0+\hat{H}_{\rm BSBS}+\hat{H}_{\rm OM}+\hat{H}_{\rm D}+\hat{H}_{\rm F}, \tag{1}$$

where

$$\begin{aligned}
\hat{H}_0 &= \sum_j \omega_j \hat{a}_j^\dagger \hat{a}_j+\omega_b\hat{b}^\dagger\hat{b}+\omega_{\rm m}\hat{c}^\dagger\hat{c},\\
\hat{H}_{\rm BSBS} &= -g_b(\hat{a}_1^\dagger\hat{a}_2\hat{b}+\hat{a}_1\hat{a}_2^\dagger\hat{b}^\dagger),\\
\hat{H}_{\rm OM} &= -\sum_j g_{c_j}\hat{a}_j^\dagger\hat{a}_j(\hat{c}+\hat{c}^\dagger),\\
\hat{H}_{\rm D} &= {\rm i}\sum_j\sqrt{\kappa_{{\rm ex}_j}\varepsilon_{d_j}}(\hat{a}_j^\dagger {\rm e}^{-{\rm i}\omega_{d_j}t}-\hat{a}_j{\rm e}^{{\rm i}\omega_{d_j}t}),\\
\hat{H}_{\rm DN} &= \frac{\eta}{2}(\hat{c}+\hat{c}^\dagger)^4.
\end{aligned} \tag{2}$$

Here, $\hat{H}_0$ is the free Hamiltonian of the system. $\hat{a}_j$ ($\hat{a}_j^\dagger$) for $j=1,2$, $\hat{b}$ ($\hat{b}^\dagger$) and $\hat{c}$ ($\hat{c}^\dagger$) are the annihilation (creation) operators of the optical mode, the Brillouin acoustic mode, and the mechanical mode, respectively. $\hat{H}_{\rm BSBS}$ is the Hamiltonian of a triply resonant phonon–photon interaction via the BSBS process, $g_b$ is the single-photon Brillouin coupling strength between two optical modes $\hat{a}_1$, $\hat{a}_2$ and a Brillouin acoustic mode $\hat{b}$. $\hat{H}_{\rm OM}$ describes the radiation-pressure coupling between the optical mode $\hat{a}_{1(2)}$ and the target mechanical mode $\hat{c}$ with a single-photon coupling strength $g_{c_{1(2)}}$. $\hat{H}_{\rm D}$ is the driving term of the optical mode $\hat{a}_{1(2)}$ with total decay rate $\kappa_{1(2)}=\kappa_{0_{1(2)}}+\kappa_{{\rm ex}_{1(2)}}$ which includes an intrinsic decay rate $\kappa_{0_{1(2)}}$ and an external decay rate $\kappa_{{\rm ex}_{1(2)}}$. $\varepsilon_{d_{1(2)}}$ and $\omega_{d_{1(2)}}$ are the amplitude and frequency of the external control field, respectively. $\hat{H}_{\rm DN}$ is the Duffing nonlinear term, the strong nonlinearity can be realized by the coupling between a mechanical mode and an ancilla system.[45–48]

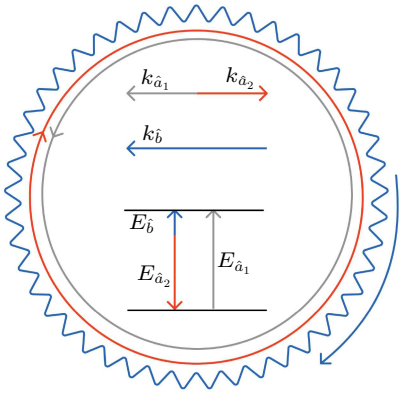



**Fig. 1.** Momentum and energy conservation in BSBS.

According to the Hamiltonian in Eq. (1), in the rotation frame with $\hat{H}_{\rm r}=\omega_{d_1}\hat{a}_1^\dagger\hat{a}_1+\omega_{d_2}\hat{a}_2^\dagger\hat{a}_2+(\omega_{d_1}-\omega_{d_2})\hat{b}^\dagger\hat{b}$, the dynamics of the cavity fields and the mechanical mode can be solved as

$$\begin{aligned}
\dot{\hat{a}}_1 &= -[{\rm i}(\omega_1-\omega_{d_1})+\kappa_1/2]\hat{a}_1+{\rm i}g_b\hat{a}_2\hat{b}\\
&\quad +{\rm i}g_{c_1}\hat{a}_1(\hat{c}+\hat{c}^\dagger)+\sqrt{\kappa_{{\rm ex}_1}}\varepsilon_{d_1}+\sqrt{\kappa_1}\hat{a}_1^{\rm in}(t),\\
\dot{\hat{a}}_2 &= -[{\rm i}(\omega_2-\omega_{d_2})+\kappa_2/2]\hat{a}_2+{\rm i}g_b\hat{a}_1\hat{b}^\dagger\\
&\quad +{\rm i}g_{c_2}\hat{a}_2(\hat{c}+\hat{c}^\dagger)+\sqrt{\kappa_{{\rm ex}_2}}\varepsilon_{d_2}+\sqrt{\kappa_2}\hat{a}_2^{\rm in}(t),
\end{aligned}$$

$$\dot{\hat{c}} = -(\mathrm{i}\omega_{\mathrm{m}} + \gamma_{\mathrm{m}}/2)\hat{c} + \mathrm{i}(g_{c_1}\hat{a}_1^{\dagger}\hat{a}_1 + g_{c_2}\hat{a}_2^{\dagger}\hat{a}_2) - 2\mathrm{i}\eta(\hat{c}+\hat{c}^{\dagger})^3 + \sqrt{\gamma_{\mathrm{m}}}\hat{c}^{\mathrm{in}}(t), \quad (3)$$

where $\hat{a}_{1(2)}^{\mathrm{in}}(t)$ and $\hat{c}^{\mathrm{in}}(t)$ are the input vacuum noise for the cavity mode $\hat{a}_{1(2)}$ and the thermal noises for the Duffing mechanical mode $\hat{c}$, respectively.

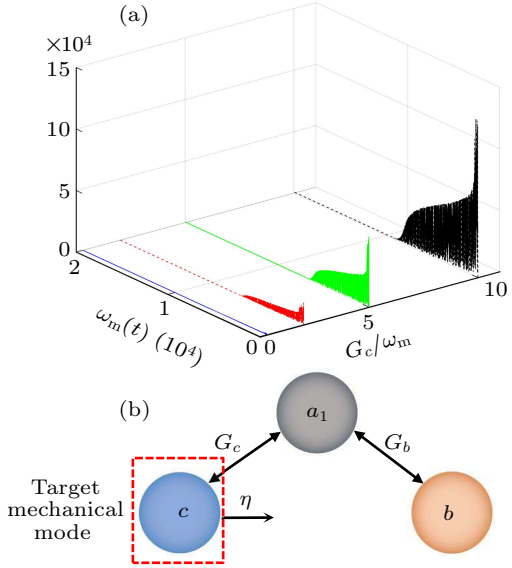



**Fig. 2.** (a) The time evolution of $|\beta|$ for different optomechanical coupling strengths $G_c$. Here we choose $\omega_{\mathrm{m}}/(2\pi) = 1$ MHz, $g_{c_1} = 10^{-4}\omega_{\mathrm{m}}$, $\kappa_1 = 0.02\omega_{\mathrm{m}}$, $\gamma_b = 0.4\omega_{\mathrm{m}}$, $\gamma_{\mathrm{m}} = 10^{-4}\omega_{\mathrm{m}}$, $\eta = 10^{-4}\omega_{\mathrm{m}}$, $n_{\mathrm{m}} = 100$, and $\kappa_{0_1} = 0$. The different optomechanical coupling strengths $G_c = 0.3\omega_{\mathrm{m}}$, $G_c = 2\omega_{\mathrm{m}}$, $G_c = 5\omega_{\mathrm{m}}$, and $G_c = 10\omega_{\mathrm{m}}$ correspond to cases ($\varepsilon_{d_1} \approx 47.68\omega_{\mathrm{m}}$, $\omega_1 - \omega_d \approx 5.65\omega_{\mathrm{m}}$), ($\varepsilon_{d_1} \approx 1.14\times10^3\omega_{\mathrm{m}}$, $\omega_1 - \omega_d \approx 20.29\omega_{\mathrm{m}}$), ($\varepsilon_{d_1} \approx 5.26\times10^3\omega_{\mathrm{m}}$, $\omega_1 - \omega_d \approx 37.41\omega_{\mathrm{m}}$ ) and ($\varepsilon_{d_1} \approx 1.67\times10^4\omega_{\mathrm{m}}$, $\omega_1 - \omega_d \approx 59.40\omega_{\mathrm{m}}$), respectively. (b) Schematic of the effective three-mode optomechanical device which consists of an optical mode $\hat{a}_1$, an acoustic mode $\hat{b}$ and a mechanical mode $\hat{c}$ (nonlinearity $\eta$). $G_c$ ($G_b$) is the effective phonon–photon coupling between the mechanical (acoustic) mode $\hat{c}$ ($\hat{b}$) and the optical mode $\hat{a}_1$, which arises from the radiation pressure (electrostrictive) force.

By using a similar method as that in Ref. [18], when the optical mode $\hat{a}_2$ is pumped by a very strong control field, in the weak coupling regime $g_b, g_{c_2} \ll \omega_b, \kappa_{1(2)}$, and the duration of control pulse satisfies $\tau_{\mathrm{p}} \gg 1/\kappa_2$, this control field can be treated classically, the influence of BSBS on the dynamical equations of $\hat{a}_1$ and $\hat{a}_2$ can be neglected, and the impact of the optomechanical interaction between the Duffing mechanical mode and optical mode can also be neglected in the weak optomechanical coupling regime when we adopt the linearization techniques, so the steady state solution $\alpha_2$ of the optical mode $\hat{a}_2$ can be obtained as

$$\alpha_2 = \frac{\sqrt{\kappa_{\mathrm{ex}_2}}\varepsilon_{d_2}}{\kappa_2/2 + \mathrm{i}\Delta_2}, \quad (4)$$

where $\Delta_2 = \omega_2 - \omega_{d_2}$. The Hamiltonian (1) of the system can be linearized as

$$\hat{H}_{\mathrm{lin}} = \Delta_1\hat{a}_1^{\dagger}\hat{a}_1 + \Delta_b\hat{b}^{\dagger}\hat{b} + \tilde{\omega}_{\mathrm{m}}\hat{c}^{\dagger}\hat{c} - [G_b\hat{a}_1^{\dagger}\hat{b} + G_c\hat{a}_1^{\dagger}(\hat{c}^{\dagger}+\hat{c}) + \mathrm{H.c.}] + \Lambda(\hat{c}^2 + \hat{c}^{\dagger 2}), \quad (5)$$

where

$$\Delta_1 = \omega_1 - \omega_{d_1} - 2g_{c_1}(\beta+\beta^*),$$
$$\Delta_b = \omega_b + \omega_{d_2} - \omega_{d_1},$$
$$\tilde{\omega}_{\mathrm{m}} = \omega_{\mathrm{m}} + 2\Lambda, \quad G_b = g_b\alpha_2,$$
$$G_c = g_{c_1}\alpha_1, \quad \Lambda = 3\eta(4|\beta|^2+1). \quad (6)$$

The average amplitudes $\alpha_1$ and $\beta$ of optical mode $\hat{a}_1$ and mechanical mode $\hat{c}$, respectively, fulfill

$$\dot{\alpha}_1 = (-\mathrm{i}\Delta_1 - \kappa_1/2)\alpha_1 + \sqrt{\kappa_{\mathrm{ex}_1}}\varepsilon_{d_1},$$
$$\dot{\beta} = (-\mathrm{i}\omega_{\mathrm{m}} - \gamma_{\mathrm{m}}/2)\beta - 2\mathrm{i}\eta(\beta^{*3} + \beta^3 + 3\beta^{*2}\beta + 3\beta^*\beta^2 + 3\beta^* + 3\beta) + \mathrm{i}g_{c_1}|\alpha_1|^2. \quad (7)$$

As shown in Fig. 2(a), we plot the time evolution of $|\beta|$ for different optomechanical coupling strengths $G_c$. This indicates that $|\beta|$ gradually tends to be stable after a period of time, so the stability of $|\beta|$ can be ensured in our scheme. In the following calculation, we focus on the steady solution of $|\beta|$, i.e., we calculate $|\beta|$ by setting $\dot{\alpha}_1 = \dot{\beta} = 0$. The effective optomechanical model used in our scheme is equivalent to a three-mode optomechanical device, as shown in Fig. 2(b).

## 3. The steady-state position fluctuation of the mechanical mode

In order to realize the steady-state mechanical squeezing of the target mechanical mode $\hat{c}$, we introduce the squeezing transformation $\hat{c} = \cosh(r)\hat{c}_s - \sinh(r)\hat{c}_s^{\dagger}$ with

$$r = \frac{1}{4}\ln(1 + 4\Lambda/\omega_{\mathrm{m}}) \quad (8)$$

to the Hamiltonian Eq. (5), where $\hat{c}_s$ is the squeezed mechanical mode, the effective Hamiltonian $\hat{H}_{\mathrm{eff}}$ of the system in the squeezing transformation frame is given by

$$\hat{H}_{\mathrm{eff}} = \Delta_1\hat{a}_1^{\dagger}\hat{a}_1 + \Delta_b\hat{b}^{\dagger}\hat{b} + \omega_{\mathrm{m}}'\hat{c}_s^{\dagger}\hat{c}_s - [G_b\hat{a}_1^{\dagger}\hat{b} + G_c'\hat{a}_1^{\dagger}(\hat{c}_s^{\dagger}+\hat{c}_s) + \mathrm{H.c.}], \quad (9)$$

where $\omega_{\mathrm{m}}' = \omega_{\mathrm{m}}\sqrt{1 + 4\Lambda/\omega_{\mathrm{m}}}$ and $G_c' = G_c(1 + 4\Lambda/\omega_{\mathrm{m}})^{-\frac{1}{4}}$ are the effective mechanical frequency and the optomechanical coupling in the squeezing transformation frame, respectively. The dynamics for the optical mode $\hat{a}_1$, the acoustic mode $\hat{b}$ and the squeezed mechanical mode $\hat{c}_s$ can be described by the quantum Langevin equations

$$\dot{\hat{a}}_1 = -\left(\frac{\kappa_1}{2} + \mathrm{i}\Delta_1\right)\hat{a}_1 + \mathrm{i}G_b\hat{b} + \mathrm{i}G_c'(\hat{c}_s^{\dagger}+\hat{c}_s) + \sqrt{\kappa_1}\hat{a}_1^{\mathrm{in}}(t),$$
$$\dot{\hat{b}} = -\left(\frac{\gamma_b}{2} + \mathrm{i}\Delta_b\right)\hat{b} + \mathrm{i}G_b^*\hat{a}_1 + \sqrt{\gamma_b}\hat{b}^{\mathrm{in}}(t),$$
$$\dot{\hat{c}}_s = -\left(\frac{\gamma_{\mathrm{m}}}{2} + \mathrm{i}\omega_{\mathrm{m}}'\right)\hat{c}_s + \mathrm{i}(G_c'\hat{a}_1^{\dagger} + G_c'^*\hat{a}_1) + \sqrt{\gamma_{\mathrm{m}}}\hat{c}_s^{\mathrm{in}}(t), \quad (10)$$

where $\gamma_b$ is the decay rate of the Brillouin acoustic mode. The input vacuum noise $\hat{a}_1^{\mathrm{in}}(t)$ for the cavity mode and the thermal noises $\hat{b}^{\mathrm{in}}(t), \hat{c}_s^{\mathrm{in}}(t)$ for the mechanical modes satisfy

$$\langle\hat{a}_1^{\mathrm{in}}(t)\hat{a}_1^{\mathrm{in}\dagger}(t')\rangle = \langle\hat{b}^{\mathrm{in}}(t)\hat{b}^{\mathrm{in}\dagger}(t')\rangle = \delta(t-t'),$$

$$\langle \hat{c}_s^{\text{in}\dagger}(t)\hat{c}_s^{\text{in}}(t')\rangle = N_{\text{eff}}\delta(t-t'),$$
$$\langle \hat{c}_s^{\text{in}}(t)\hat{c}_s^{\text{in}}(t')\rangle = M_{\text{eff}}\delta(t-t'), \tag{11}$$

where

$$N_{\text{eff}} = \cosh(2r)n_{\text{m}} + \sinh^2(r),$$
$$M_{\text{eff}} = \sinh(2r)(n_{\text{m}} + 1/2),$$

$n_{\text{m}} = [\exp(\hbar\omega_{\text{m}}/(k_{\text{B}}T)) - 1]^{-1}$ is the equilibrium phonon occupation, $k_{\text{B}}$ is the Boltzmann constant, and we have neglected the thermal noise of the high-frequency Brillouin mode $\hat{b}$ due to $\omega_b \gg \omega_{\text{m}}$. To calculate the position variance of the mechanical mode $\hat{c}$, we define the column vectors which contain the amplitude and phase quadrature operators $\hat{X}_o = (\hat{o} + \hat{o}^\dagger)/\sqrt{2}$, $\hat{P}_o = \text{i}(\hat{o}^\dagger - \hat{o})/\sqrt{2}$ and the corresponding noise quadrature operators $\hat{X}_o^{\text{in}} = (\hat{o}^{\text{in}} + \hat{o}^{\dagger\text{in}})/\sqrt{2}, \hat{P}_o^{\text{in}} = \text{i}(\hat{o}^{\text{in}\dagger} - \hat{o}^{\text{in}})/\sqrt{2}$ ($o = a_1, b, c_s$) for the fluctuations $D = [\hat{X}_{\hat{a}_1}, \hat{P}_{\hat{a}_1}, \hat{X}_{\hat{b}}, \hat{P}_{\hat{b}}, \hat{X}_{\hat{c}_s}, \hat{P}_{\hat{c}_s}]^{\text{T}}$ and the quantum noises $D^{\text{in}} = [\hat{X}_{\hat{a}_1}^{\text{in}}, \hat{P}_{\hat{a}_1}^{\text{in}}, \hat{X}_{\hat{b}}^{\text{in}}, \hat{P}_{\hat{b}}^{\text{in}}, \hat{X}_{\hat{c}_s}^{\text{in}}, \hat{P}_{\hat{c}_s}^{\text{in}}]^{\text{T}}$. Then, the evolution of the system in Eq. (10) can be formulated as

$$\frac{\text{d}D}{\text{d}t} = MD + D^{\text{in}} \tag{12}$$

with a $6\times 6$ matrix

$$M = \begin{bmatrix} -\frac{\kappa_1}{2} & \Delta_1 & 0 & -G_b & 0 & 0 \\ -\Delta_1 & -\frac{\kappa_1}{2} & G_b & 0 & 2G_c' & 0 \\ 0 & -G_b & -\frac{\gamma_b}{2} & \Delta_b & 0 & 0 \\ G_b & 0 & -\Delta_b & -\frac{\gamma_b}{2} & 0 & 0 \\ 0 & 0 & 0 & 0 & -\frac{\gamma_{\text{m}}}{2} & \omega_{\text{m}}' \\ 2G_c' & 0 & 0 & 0 & -\omega_{\text{m}}' & \frac{\gamma_{\text{m}}}{2} \end{bmatrix}. \tag{13}$$

Here, the coupling constants $G_b$ and $G_c'$ have been chosen as real numbers for simplicity. The stability of the system can be ensured when all the eigenvalues of $M$ have negative real parts. We have checked carefully the stability of the system in the following calculation.

The linearized Hamiltonian and the zero-mean Gaussian nature of the quantum noises ensure the Gaussian characteristics of the system, the time evolution of the system can be described by a $6\times 6$ covariance matrix $V$ with elements $V_{kl} = \langle D_k D_l + D_l D_k\rangle/2$ ($k, l = 1, 2, 3, 4, 5, 6$), and the motion equations in Eq. (12) can be expressed as

$$\frac{\text{d}V}{\text{d}t} = MV + VM^{\text{T}} + A, \tag{14}$$

where the diagonal noise correlation matrix

$$A = \text{Diag}\left[\frac{\kappa_1}{2}, \frac{\kappa_1}{2}, \frac{\gamma_b}{2}, \frac{\gamma_b}{2}, \frac{\text{e}^{2r}\gamma_{\text{m}}(2n_{\text{m}}+1)}{2}, \frac{\text{e}^{-2r}\gamma_{\text{m}}(2n_{\text{m}}+1)}{2}\right].$$

When the system reaches a steady state for $t \to \infty$, we obtain a Lyapunov equation

$$MV(\infty) + V(\infty)M^{\text{T}} = -A, \tag{15}$$

the steady-state position variance $\langle \delta\hat{X}_{\hat{c}}^2\rangle$ of the mechanical mode $\hat{c}$ in the original frame can be obtained as

$$\langle \delta\hat{X}_{\hat{c}}^2\rangle = \text{e}^{-2r}V_{55}, \tag{16}$$

the corresponding effective phonon number $n_{\text{eff}}$ of the mechanical oscillator $\hat{c}$ in the original frame reads

$$n_{\text{eff}} = (\text{e}^{-2r}V_{55} + \text{e}^{2r}V_{66} - 1)/2. \tag{17}$$

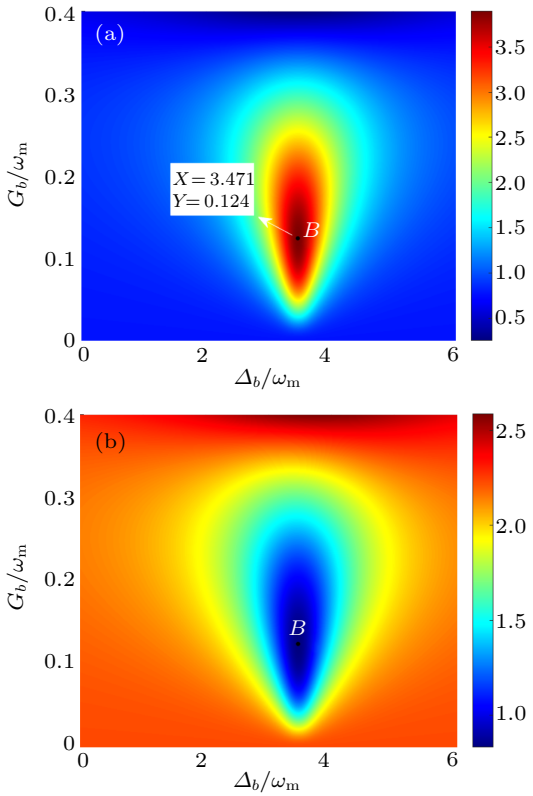



**Fig. 3.** Position variance $\langle \delta\hat{X}_{\hat{c}}^2\rangle$ (dB) (a) and effective phonon number $n_{\text{eff}}$ (b) of the mechanical mode $\hat{c}$ as a function of effective coupling $G_b$ and frequency detuning $\Delta_b$. Here, we choose $G_c = 0.15\omega_{\text{m}}$, $\Delta_1 = \omega_{\text{m}}'$, the other parameters are the same as in Fig. 2(a).

To evaluate the squeezing degree of the mechanical mode, we adopt the physical quantity $\langle \delta\hat{X}_{\hat{c}}^2\rangle$ (dB) $= -10\log_{10}\frac{\langle \delta\hat{X}_{\hat{c}}^2\rangle}{\langle \delta\hat{X}_{\hat{c}}^2\rangle_{\text{vac}}}$ in the following calculations, where $\langle \delta\hat{X}_{\hat{c}}^2\rangle_{\text{vac}} = 1/2$ is the position variance of the mechanical oscillator in the ground state. From now on, we study the effect of the phonon–photon interaction via the BSBS process on the position variance $\langle \delta\hat{X}_{\hat{c}}^2\rangle$ (dB) of the mechanical mode $\hat{c}$. Here, we choose the red-detuned resonance $\Delta_1 = \omega_{\text{m}}'$ to cool the squeezed mechanical mode $\hat{c}_s$ by suppressing the heating terms $G_c'(\hat{a}_1^\dagger\hat{c}_s^\dagger + \hat{a}_1\hat{c}_s)$. As shown in Fig. 3(a), we plot the effects of the frequency detuning $\Delta_b$ and the effective phonon–photon coupling $G_b$ on the position variance $\langle \delta\hat{X}_{\hat{c}}^2\rangle$ (dB) of the mechanical mode $\hat{c}$. The strongest squeezing appears at the resonant point $B$ ($\Delta_b = 3.471\omega_{\text{m}} = \Delta_1$ and $G_b = 0.124\omega_{\text{m}}$). Because there is a most effective beam splitter-type coupling at this resonance point, the BSBS is an anti-Stokes process. Then, the introduction of the phonon–photon interaction via the BSBS process provides an extra loss channel to cool the

OMS.[18] It can be seen clearly from Fig. 3(b) that a minimum effective phonon number $n_{\rm eff}$ appears at point $B$. And finally, an optimal cooling effect can be obtained. Cooling is essential for the preparation of the mechanical squeezing, so optimal squeezing is achieved at point $B$. It is clear that the effective coupling $G_b$ also has an obvious influence on the position variance of the mechanical mode, and optimal squeezing can be obtained when a proper $G_b$ is chosen. Additionally, the optimal choice of $G_b$ is related to the effective optomechanical coupling $G_c$, which can be further depicted in Fig. 4(a).

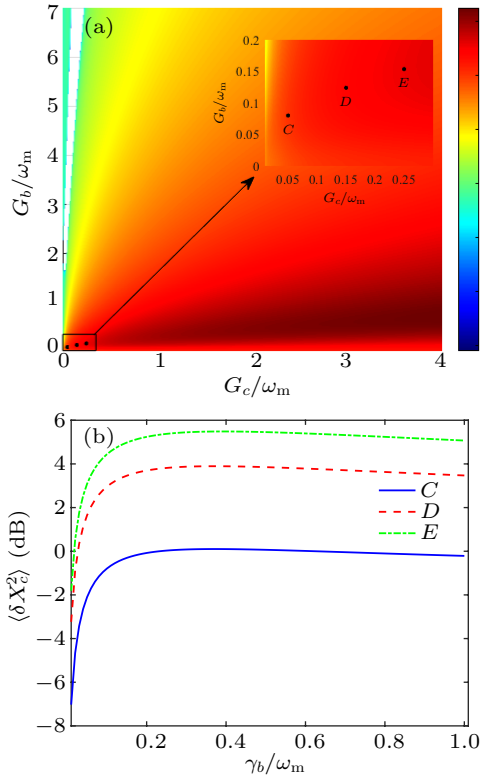



**Fig. 4.** (a) Position variance $\langle\delta\hat{X}_{\hat{c}}^2\rangle$ (dB) of the mechanical mode $\hat{c}$ versus the optomechanical coupling $G_c$ and the effective phonon–photon coupling $G_b$ via the BSBS process. (b) Position variance $\langle\delta\hat{X}_{\hat{c}}^2\rangle$ of the mechanical mode versus the Brillouin acoustic damping rate $\gamma_b$ at points $C$, $D$, and $E$ in Fig. 3(a). The inset presents a zoom in on the tiny red region. The white region in (a) shows the system's unstable behavior. Here, we choose $\Delta_b = \Delta_1 = \omega_{\rm m}'$, the other parameters are the same as Fig. 2(a).

In Fig. 4(a), we plot the position variance $\langle\delta\hat{X}_{\hat{c}}^2\rangle$ (dB) of the mechanical mode $\hat{c}$ versus the couplings $G_c$ and $G_b$ when $\Delta_b = \Delta_1 = \omega_{\rm m}'$. It is clear that the position squeezing is first enhanced and then weakened with the increasing of the effective phonon–photon coupling $G_b$ for a fixed $G_c$. For a given and strong $G_b$, the squeezing degree of the mechanical mode is proportional to the optomechanical coupling $G_c$. When $G_b$ is not very strong, an optimal squeezing is obtained with increase of $G_c$. The physical mechanics can be explained as follows. When $G_b$ is not very strong, and the optomechanical interaction $G_c'$ between the optical mode $\hat{a}_1$ and the squeezed mechanical mode $\hat{c}_s$ can be neglected in the weak-coupling regime $G_c \ll 0.01\omega_{\rm m}$, then the effective Hamiltonian is expressed as $\hat{H}_{\rm eff}' = \Delta_1\hat{a}_1^\dagger\hat{a}_1 + \Delta_b\hat{b}^\dagger\hat{b} - G_b(\hat{a}_1\hat{b}^\dagger + \hat{a}_1^\dagger\hat{b})$, and the fluctuation spectrum $S_{FF}(\omega) = \int {\rm d}t\, {\rm e}^{{\rm i}\omega t}\langle\hat{F}(t)\hat{F}(0)\rangle$ of the radiation-pressure force $F = \hat{a}_1^\dagger + \hat{a}_1$ can be derived as

$$S_{FF}(\omega) = \frac{\dfrac{|G_b|^2\gamma_b}{|\frac{\gamma_b}{2} - {\rm i}(\omega-\Delta_b)|^2} + \kappa_1}{\left|\dfrac{\kappa_1}{2} - {\rm i}(\omega-\Delta_1) + \dfrac{|G_b|^2}{\frac{\gamma_b}{2} - {\rm i}(\omega-\Delta_b)}\right|^2}. \tag{18}$$

According to the rate equation,[22,49] we obtain the final effective phonon number $n_{\rm eff}^s$ of the mechanical oscillator $\hat{c}_s$ in the squeezing frame as

$$n_{\rm eff}^s = \langle\hat{c}_s^\dagger\hat{c}_s\rangle = \frac{\gamma_{\rm m}N_{\rm eff} + \gamma_c n_c}{\gamma_{\rm m}+\gamma_c} \approx \frac{\gamma_{\rm m}N_{\rm eff}}{\gamma_{\rm m}+\gamma_c}, \tag{19}$$

with

$$\begin{aligned}
\gamma_c &= G_c'^2[S_{FF}(+\omega_{\rm m}') - S_{FF}(-\omega_{\rm m}')] \approx \frac{4G_c'^2}{\kappa_{\rm eff}},\\
\kappa_{\rm eff} &= \kappa_1 + \frac{4|G_b|^2}{\gamma_b},\\
n_c &= \frac{S_{FF}(-\omega_{\rm m}')}{S_{FF}(+\omega_{\rm m}') - S_{FF}(-\omega_{\rm m}')},
\end{aligned} \tag{20}$$

and $n_{\rm eff} = \langle\hat{c}^\dagger\hat{c}\rangle$ in the original frame

$$n_{\rm eff} = \cosh(2r)n_{\rm eff}^s + \sinh^2(r), \tag{21}$$

under the resonance condition $\Delta_1 = \Delta_b = \omega_{\rm m}'$. Here, we have used the approximations $\gamma_{\rm m} \ll \kappa_1 \ll \gamma_b \ll \omega_{\rm m}'$ and $S_{FF}(-\omega_{\rm m}') \ll S_{FF}(\omega_{\rm m}')$. The corresponding position variance of the mechanical mode in the original frame can be calculated as

$$\langle\delta\hat{X}_{\hat{c}}^2\rangle = \left(n_{\rm eff}^s + \frac{1}{2}\right){\rm e}^{-2r}. \tag{22}$$

From Eqs. (19) and (22), it is clear that the final phonon number $n_{\rm eff}$ and the squeezing parameter $r$ which is proportional to $|\beta|$ are two key parameters in preparing the mechanical squeezing. Larger $r$ or smaller $n_{\rm eff}$ are beneficial for generating stronger mechanical squeezing. In the weak optomechanical coupling regime, the linewidth $\kappa_{\rm eff}$ of the optical mode $\hat{a}_1$ is broadened with the increase of the effective phonon–photon coupling $G_b$ via the BSBS process, which leads to the increase of the final phonon number $n_{\rm eff}$, the ground-state cooling effect of the mechanical motion becomes worse, while the squeezing parameter $r$ is independent of $G_b$, so the squeezing degree of the position of the mechanical mode $\hat{c}$ decreases. Interestingly, when we enter into a large optomechanical coupling region $G_c \geq 0.01\omega_{\rm m}$ and $G_b$ is not very strong, the mechanical squeezing is enhanced greatly with increasing $G_b$. However, a very strong $G_b$ is harmful to the enhancement of the mechanical squeezing, which originates from the emergence of the supermodes $\hat{a}_+ = (\hat{a}_1 + \hat{b})/\sqrt{2}$ with frequency $\omega_{\hat{a}_+} = \Delta_1 - |G_b|$ and $\hat{a}_- = (\hat{b} - \hat{a}_1)/\sqrt{2}$ with frequency $\omega_{\hat{a}_-} = \Delta_1 + |G_b|$, the

interaction term $G_c'(\hat{a}_+^\dagger \hat{c}_s^\dagger + c_s \hat{a}_+)$ cannot be omitted. When $G_b$ is not very strong and given, the increase of the weak optomechanical coupling $G_c$ leads to a larger $\gamma_c$ in Eq. (19) and $|\beta|$, a larger cooling rate and squeezing parameter $r$ are obtained, the squeezing degree of the mechanical mode is improved rapidly at the beginning. Whereas the non-resonant term $G_c'(\hat{a}_1 \hat{c}_s + \hat{a}_1^\dagger \hat{c}_s^\dagger)$ cannot be ignored when the coupling $G_c$ is large enough, the cooling effect is bad again, so the squeezing degree of the mechanical mode increases more and more slowly. Based on the above analysis, we conclude that an optimal mechanical squeezing is achievable when the optomechanical coupling $G_c$ and the effective phonon–photon coupling $G_b$ caused by the BSBS are chosen properly, for example, as shown in the inset of Fig. 4(a), at the points $C$ ($G_c = 0.050\omega_\mathrm{m}, G_b = 0.08\omega_\mathrm{m}$), $D$ ($G_c = 0.150\omega_\mathrm{m}, G_b = 0.124\omega_\mathrm{m}$) and $E$ ($G_c = 0.250\omega_\mathrm{m}, G_b = 0.154\omega_\mathrm{m}$), the optimal mechanical squeezing degrees are 0.099, 3.892, and 5.486, respectively.

In the BSBS, the Brillouin acoustic mode has a large decay rate, which is a key factor in our scheme. In the above discussions, we have used the condition $\gamma_b \gg \kappa_1$. To confirm the necessity of this condition, as shown in Fig. 4(b), we plot the position variance $\langle \delta \hat{X}_{\hat{c}}^2 \rangle$ of the mechanical mode versus the Brillouin acoustic decay rate $\gamma_b$ at points $C$, $D$, and $E$ in Fig. 4(a). Obviously, the squeezing degree grows rapidly to a maximum and then decreases slightly as the acoustic damping rate $\gamma_b$ increases. The strongest squeezing at points $C$, $D$, and $E$ all appear in the region where $\gamma_b \gg \kappa_1 = 0.02\omega_\mathrm{m}$.

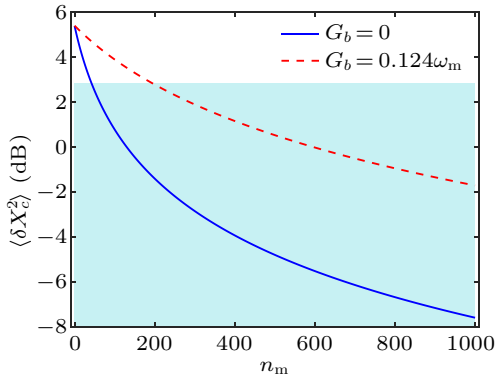



**Fig. 5.** Position variance $\langle \delta \hat{X}_{\hat{c}}^2 \rangle$ of the mechanical mode $\hat{c}$ as a function of the thermal phonon number $n_\mathrm{m}$ for $G_b = 0$ (black solid line) and $G_b = 0.124\omega_\mathrm{m}$ (red dashed line). Here we choose $\Delta_b = \Delta_1 = \omega_\mathrm{m}'$, the other parameters are the same as in Fig. 2(a). The shadowed blue bottom region corresponds to squeezing below the 3 dB limit.

To examine the effect of the mechanical thermal noises, we plot the position variance $\langle \delta \hat{X}_{\hat{c}}^2 \rangle$ (dB) of the mechanical mode as a function of the thermal phonon number $n_\mathrm{m}$ in Fig. 5. Intuitively, the thermal phonon number has a negative influence on the generation of the mechanical squeezing. When $n_\mathrm{m} \neq 0$, the introduction of the effective phonon–photon coupling $G_b$ (red dashed line) contributes to the cooling of the target mechanical oscillator, the mechanical squeezing is enhanced greatly, and the robustness of the mechanical squeezing to the thermal noise of the mechanical environment can be greatly improved compared with the case without the effective coupling $G_b = 0$ (blue solid line).

In Fig. 6, we plot the position variance $\langle \delta \hat{X}_{\hat{c}}^2 \rangle$ (dB) of the mechanical mode $\hat{c}$ as a function of the Duffing nonlinearity amplitude $\eta$ for $G_b = 0$ (blue solid line) and $G_b = 0.124\omega_\mathrm{m}$ (red dashed line). As seen, the squeezing degree can be further improved when a proper effective phonon–photon coupling caused by the BSBS $G_b = 0.124\omega_\mathrm{m}$ is introduced compared to the case without the BSBS $G_b = 0$. For example, for a weak nonlinearity $\eta = 0.25 \times 10^{-4}\omega_\mathrm{m}$, the squeezing degree $\langle \delta \hat{X}_{\hat{c}}^2 \rangle = 3.17$ dB at point $G$ still exceeds the 3 dB limit (as the red line above the shadowed blue region shows) in the case of $G_b = 0.124\omega_\mathrm{m}$, which is about 13 times that $\langle \delta \hat{X}_{\hat{c}}^2 \rangle = 0.248$ dB at point $F$ when $G_b = 0$. In addition, it is clear that the Duffing nonlinearity is necessary for the generation of mechanical squeezing. The introduction of BSBS mainly provides a cooling path for the OMS, enhancing mechanical squeezing, but the mechanical squeezing is primarily generated by the Duffing nonlinearity.

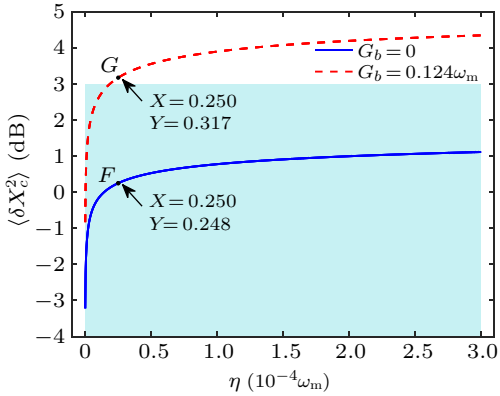



**Fig. 6.** Position variance $\langle \delta \hat{X}_{\hat{c}}^2 \rangle$ of the mechanical mode $\hat{c}$ as a function of the Duffing nonlinearity amplitude $\eta$ for $G_b = 0$ (blue solid line) and $G_b = 0.124\omega_\mathrm{m}$ (red dashed line). Here, we choose $\Delta_b = \Delta_1 = \omega_\mathrm{m}'$, the other parameters are the same as in Fig. 2(a). The shadowed blue bottom region corresponds to squeezing below the 3 dB limit.

## 4. Discussion and conclusion

Our optomechanical model can be realized based on advanced experimental technology. First, the triply resonant phonon–photon interaction via the BSBS process has been achieved experimentally in the platform of whispering-gallery-mode OMS,[19] and the frequency of the Brillouin acoustic mode has reached about 10 GHz,[19] which indicates that it is reasonable to ignore the thermal noises of the acoustic mode, and the Brillouin acoustic mode with large decay rate has proven to be effective for the cooling of the target mechanical oscillator.[18] Second, we choose $\omega_\mathrm{m}/2\pi = 1$ MHz and $g_{c_1} = 10^{-4}\omega_\mathrm{m} = 2\pi \times 100$ Hz in the scheme.

In fact, the single-photon optomechanical coupling strength $g_{c_1}/2\pi \sim 100$ Hz can be obtained by using a nanomechanical string oscillator with a resonance frequency in the MHz range ($\omega_{\rm m}/2\pi \sim 1$ MHz) coupled to a silica microtoroid.[50] The preparation of the Duffing nonlinearity has been investigated in Refs. [45–48], and the amplitude $\eta = 10^{-4}\omega_{\rm m}$ is achievable.[28] Third, to reduce the negative effect of the quantum noises, it is necessary to precool the system,[51] and the related measurements can be performed via the dilution refrigeration or the sideband cooling cooling.[31,51–53] Finally, mechanical squeezing can be detected by homodyning the output field of the ancilla mode with a local oscillator.[54]

We have proposed an optomechanical scheme for preparing a strong steady-state mechanical squeezing via BSBS. When the effective frequency detuning of the Brillouin acoustic mode equals that of the optical mode, and the optomechanical coupling and the phonon–photon coupling via the BSBS process are selected reasonably, the introduction of the phonon–photon interaction enables the enhancement of mechanical squeezing under the red-detuning resonant condition in the squeezing transformation frame. In the weak optomechanical coupling regime, the increase of the effective phonon–photon coupling caused by the BSBS broadens the linewidth of the optical mode, the cooling efficiency of the mechanical mode decreases, and the mechanical squeezing becomes worse. However, for a strong optomechanical coupling, the mechanical squeezing can be enhanced effectively in the presence of the phonon–photon coupling via the BSBS process. However, the very strong phonon–photon coupling leads to the emergence of supermodes, which are harmful to the phonon cooling and the squeezing degree reduces. When the Duffing nonlinearity is weak, compared to the case without the BSBS, the mechanical squeezing prepared in the presence of the BSBS is more robust to quantum noises and the squeezing degree can be improved by more than an order of magnitude.

## Acknowledgements

Project supported by the Scientific and Technological Research Program of Chongqing Municipal Education Commission (Grant No. KJQN202400624), the Natural Science Foundation of Chongqing CSTC (Grant No. CSTB2022NSCQ-BHX0020), the China Electronics Technology Group Corporation 44th Research Institute (Grant No. 6310001-2), the Project Grant "Noninvasive Sensing Measurement based on Terahertz Technology" from Province and MOE Collaborative Innovation Centre for New Generation Information Networking and Terminals, the Key Research Program of CQUPT on Interdisciplinary and Emerging Field (A2018-01), and the Venture & Innovation Support program for Chongqing Overseas Returnees Year 2022.

## References

[1] Shen Y R and Bloembergen N 1965 *Phys. Rev.* **137** A1787
[2] Yariv A 1965 *IEEE Journal of Quantum Electronics* **1** 28
[3] Cheng R J, Li X X, Wang Q, Liu D J, Huang Z M, Lv S Y, Zhou T Z, Zhang S T, Li X M and Chen Z J 2024 *Chin. Phys. B* **33** 015206
[4] He X, Harris G I, Baker C G, Sawadsky A, Sfendla Y L, Sachkou Y P, Forstner S and Bowen W P 2020 *Nat. Phys.* **16** 417
[5] Lin G, Diallo S, Saleh K, Martinenghi R, Beugnot J C, Sylvestre T and Chembo Y K 2014 *Appl. Phys. Lett.* **105** 231103
[6] Honda Y, Yoshiki W, Tetsumoto T, Fujii S, Furusawa K, Sekine N and Tanabe T 2018 *Appl. Phys. Lett.* **112** 201105
[7] Bai Y, Zhang M, Shi Q, Ding S, Qin Y, Xie Z, Jiang X and Xiao M 2021 *Phys. Rev. Lett.* **126** 063901
[8] Li J, Suh M G and Vahala K 2017 *Optica* **4** 346
[9] Bahl G, Tomes M, Marquardt F and Carmon T 2012 *Nat. Phys.* **3** 203
[10] Savchenkov A, Matsko A, Ilchenko V, Seidel D and Maleki L 2011 *Opt. Lett.* **36** 3338
[11] Bahl G, Zehnpfennig J, Tomes M and Carmon T 2011 *Nat. Commun.* **2** 403
[12] Dong C H, Shen Z, Zou C L, Zhang Y L, Fu W and Guo G C 2015 *Nat. Commun.* **6** 6193
[13] Grudinin I S, Matsko A B and Maleki L 2009 *Phys. Rev. Lett.* **102** 043902
[14] Tomes M and Carmon T 2009 *Phys. Rev. Lett.* **102** 113601
[15] Enzian G, Szczykulska M, Silver J, Del Bino L, Zhang S, Walmsley I A, Del'Haye P and Vanner M R 2019 *Optica* **6** 7
[16] Enzian G, Price J J, Freisem L, Nunn J, Janousek J, Buchler B C, Lam P K and Vanner M R 2021 *Phys. Rev. Lett.* **126** 033601
[17] Nunnenkamp A, Sudhir V, Feofanov A, Roulet A and Kippenberg T 2014 *Phys. Rev. Lett.* **113** 023604
[18] Zhang Y L, Yang C S, Shen Z, Dong C H, Guo G C, Zou C L and Zou X B 2020 *Phys. Rev. A* **101** 063836
[19] Shen Z, Zhang Y L, Zou C L, Guo G C and Dong C H 2021 *Phys. Rev. Lett.* **126** 163604
[20] Kippenberg T J and Vahala K J 2008 *Science* **321** 1172
[21] Aspelmeyer M, Meystre P and Schwab K 2012 *Physics Today* **65** 29
[22] Aspelmeyer M, Kippenberg T J and Marquardt F 2014 *Rev. Mod. Phys.* **86** 1391
[23] Chen S S, Zhang H, Song X K, Deng F G, Wang H B and Yang G J 2018 *Annalen der Physik* **530** 1800239
[24] Chen S S, Zhang H, Ai Q and Yang G J 2019 *Phys. Rev. A* **100** 052306
[25] Huang S and Agarwal G 2011 *Phys. Rev. A* **83** 043826
[26] Weis S, Rivière R, Deléglise S, Gavartin E, Arcizet O, Schliesser A and Kippenberg T J 2010 *Science* **330** 1520
[27] Safavi-Naeini A H, Alegre T M, Chan J, Eichenfield M, Winger M, Lin Q, Hill J T, Chang D E and Painter O 2011 *Nature* **472** 69
[28] Lü X Y, Liao J Q, Tian L and Nori F 2015 *Phys. Rev. A* **91** 013834
[29] Liao J Q, Law C, *et al.* 2011 *Phys. Rev. A* **83** 033820
[30] Chen S S, Meng S S, Deng H and Yang G J 2021 *Annalen der Physik* **533** 2000343
[31] Teufel J D, Donner T, Li D, Harlow J W, Allman M, Cicak K, Sirois A J, Whittaker J D, Lehnert K W and Simmonds R W 2011 *Nature* **475** 359
[32] Meenehan S M, Cohen J D, MacCabe G S, Marsili F, Shaw M D and Painter O 2015 *Phys. Rev. X* **4** 041002
[33] Clark J B, Lecocq F, Simmonds R W, Aumentado J and Teufel J D 2017 *Nature* **541** 191
[34] Caves C M, Thorne K S, Drever R W, Sandberg V D and Zimmermann M 1980 *Rev. Mod. Phys.* **52** 341
[35] LaHaye M, Buu O, Camarota B and Schwab K 2004 *Science* **304** 74
[36] Braunstein S L and Van Loock P 2005 *Rev. Mod. Phys.* **77** 513
[37] Jähne K, Genes C, Hammerer K, Wallquist M, Polzik E and Zoller P 2009 *Phys. Rev. A* **79** 063819
[38] Huang S and Agarwal G 2010 *Phys. Rev. A* **82** 033811
[39] Kronwald A, Marquardt F and Clerk A A 2013 *Phys. Rev. A* **88** 063833

[40] Wollman E E, Lei C, Weinstein A, Suh J, Kronwald A, Marquardt F, Clerk A A and Schwab K 2015 *Science* **349** 952
[41] Zhang R, Fang Y, Wang Y Y, Chesi S and Wang Y D 2019 *Phys. Rev. A* **99** 043805
[42] Mari A and Eisert J 2009 *Phys. Rev. Lett.* **103** 213603
[43] Schmidt M, Ludwig M and Marquardt F 2012 *New J. Phys.* **12** 125005
[44] Bai C H, Wang D Y, Zhang S, Liu S and Wang H F 2019 *Photonics Research* **7** 1229
[45] Blencowe M 2004 *Physics Reports* **395** 159
[46] Xiang Z L, Ashhab S, You J and Nori F 2013 *Rev. Mod. Phys.* **85** 623
[47] Jacobs K and Landahl A J 2009 *Phys. Rev. Lett.* **103** 067201
[48] Tian L 2011 *Phys. Rev. B* **84** 035417
[49] Guo Y, Li K, Nie W and Li Y 2014 *Phys. Rev. A* **90** 053841
[50] Gorodetksy M, Schliesser A, Anetsberger G, Deleglise S and Kippenberg T J 2010 *Opt. Express* **18** 23236
[51] Park Y S and Wang H 2009 *Nat. Phys.* **5** 489
[52] Schliesser A, Arcizet O, Rivière R, Anetsberger G and Kippenberg T J 2009 *Nat. Phys.* **5** 509
[53] Chan J, Alegre T M, Safavi-Naeini A H, Hill J T, Krause A, Gröblacher S, Aspelmeyer M and Painter O 2011 *Nature* **478** 89
[54] Vitali D, Gigan S, Ferreira A, Böhm H, Tombesi P, Guerreiro A, Vedral V, Zeilinger A and Aspelmeyer M 2007 *Phys. Rev. Lett.* **98** 030405